Controlled mineralisation and recrystallisation of brushite within alginate hydrogels

Sindre H. Bjørnøy[1], David Bassett[1], Seniz Ucar[2], Jens-Petter Andreassen[2], Pawel Sikorski[1]

[1] Department of Physics, Norwegian University of Science and Technology, Trondheim, Norway
[2] Department of Chemical Engineering, Norwegian University of Science and Technology, Norway

E-mail: pawel.sikorski@ntnu.no

Abstract. Due to high solubility and resorption behaviour under physiological conditions, brushite ($CaHPO_4 \cdot 2H_2O$, calcium monohydrogen phosphate dihydrate, dicalcium phosphate dihydrate) has great potential in bone regeneration applications, both in combination with scaffolds or as component of calcium phosphate cements. The use of brushite in combination with hydrogels opens possibilities for new cell based tissue engineering applications of this promising material. However, published preparation methods of brushite composites, in which the mineral phase is precipitated within the hydrogel network, fail to offer the necessary degree of control over mineral phase, content and distribution within the hydrogel matrix. The main focus of this study was to address these shortcomings by determining precise fabrication parameters needed to prepare composites with controlled composition and properties. Composite alginate microbeads were prepared using a counter-diffusion technique which allows for simultaneous crosslinking of the hydrogel and precipitation of an inorganic mineral phase. Reliable nucleation of a desired mineral phase within the alginate network proved more challenging than simple aqueous precipitation. This was largely due to ion transport within the hydrogel producing concentration gradients that modified levels of supersaturation and favoured the nucleation of other phases such as hydroxyapatite and octacalcium phosphate which would otherwise not form. To overcome this, incorporation of brushite seed crystals resulted in good control over the mineral phase and by adjusting the amount of seeds and precursor concentration, the amount of mineral could be tuned. The material has been characterized with a range of physical techniques, including scanning electron microscopy, powder X-ray diffraction and Rietveld refinement, Fourier transform infrared spectroscopy and thermogravimetric analysis, in order to assess mineral morphology, phase and amount within the organic matrix. The mineral content of the composite material converted from brushite into hydroxyapatite when submerged in simulated body fluid, indicating possible bioactivity. Additionally, initial cell culture studies revealed that both the material and the synthesis procedure is compatible with cells relevant to bone tissue engineering.

Submitted to: *Biomed. Mater.*

1. Introduction

In cell-based tissue engineering (TE) there is a need for synthetic materials that can act as scaffolds for cells. These materials must be biocompatible, preferably biodegradable and be able to provide an environment that ensures attachment, proliferation and sustained function of specific cell types[1,2]. For bone TE, an ideal scaffold should have appropriate mechanical properties, provide an environment for nutrient and growth factor exchange and have a certain porosity for cell migration and vascularisation.[3] Hydrogels are a class of polymeric networks capable of retaining large amounts of water and have shown good promise as TE scaffolds.[4,5] Their hydrated form allows for diffusion of nutrients and delivery of bioactive agents, but the high water content also means that hydrogels are inherently soft materials with low mechanical strength and are therefore more suitable for soft tissues.[6] However, hydrogel based scaffolds do possess the potential as non-invasive, injectable temporary scaffolds which can deliver cells, growth factors, drugs or combinations of these to a damaged site.[7] Hydrogels can also be used in combination with load-bearing structures in order to promote the growth of new healthy bone and aid in overcoming some of the challenges of metal implants i.e. corrosion or implant rejection.[8,9]

Human bone tissue consists mainly of hydroxyapatite (HAp) nanocrystals in an ordered collagen matrix. The interplay between the stiff, but brittle inorganic phase and the soft, but tough organic phase, combined with a hierarchical design provides the extraordinary mechanical strength of this natural composite.[10] Adding an inorganic phase, such as HAp, to a hydrogel is one approach to improve mechanical properties of the biomaterial, although so far the level required for load-bearing applications has not been reached.[11–16] However, cell response to mechanical stimuli has gained attention lately and tuning the mechanical properties of a scaffold may hold great potential.[17] It has also been shown that alginate mineralised with HAp improves cell adhesion, and the mineral itself can act as an osteoconductive surface.[18–20]

For many years HAp has been the calcium phosphate (CaP) phase of choice for application in bone augmentation procedures owing to its likeness to natural bone mineral and stability under physiological conditions. There are, however several other CaP phases that may dissolve or transform *in vivo* to allow or encourage natural remodelling procedures, thereby creating a bioactive implant. Both brushite ($CaHPO_4{\cdot}2H_2O$) and octacalcium phosphate (OCP) have been suggested as natural precursor phases to HAp, although *in vivo* evidence of this is rarely found.[21] Brushite has over the past two decades received a great deal of attention as a potential bioceramic in repair of osseous tissue.[22,23] The solubility of brushite is higher than that of HAp and OCP(pK_{sp} of 6.6, 58.6 and 48.7, respectively, at 37^oC)[24] and it therefore transforms readily into these phases at physiological conditions. The increased solubility offers a considerable advantage over alternative calcium phosphate based materials as it may provide the space and necessary ions for natural bone remodeling and regeneration.[23] It has also been shown that the resorption rate of brushite is higher than for HAp.[25] There are however some issues with the long-term fate of large volumes of implanted brushite, as it has been shown to transform into more stable phases like OCP and HAp.[26,27] This effect seems to be site-specific and is likely related to the *in vivo* fluid exchange in the sample location.[28,29] Such behavior has implications for the choice of brushite to fill large bone lesions. Interest in brushite as a biomaterial is mounting and while there are many examples of promising HAp-alginate composites, there is very little literature regarding brushite in combination with hydrogels. Brushite powder has been incorporated in an alginate matrix for fertilizer purposes and the recrystallisation of brushite in alginate at a cement-hydrogel interface has been studied by Raman-spectroscopy.[30,31] A recent attempt was made by Amer *et al.* to precipitate brushite *in situ* with alginate.[32] While mineral was formed within the hydrogel, little attention was paid to reaction conditions or biocompatibility which resulted in poorly defined composites and unstable gels. During preliminary experiments, we found that taking such an approach to the synthesis of a brushite alginate composite was unsatisfactory in terms of reaction control and reproducibility. Therefore we sought to improve this synthesis by controlling inherently dynamic reaction conditions of pH by using appropriate buffers and employed crystal seeds as a means to encourage growth of phase pure brushite within the alginate matrix without recourse to use extreme reaction conditions that would be toxic to cells.[33]

The driving force for nucleation and growth of a specific phase in solution is the supersaturation *i.e.* the difference in chemical potential of a molecule in the solution and one in the crystal.[34] According to the literature, brushite is thermodynamically stable below *ca* pH 4, but due to the nucleation and growth kinetics of different CaP phases, brushite can be precipitated at higher pH.[35,36] However, it has been seen that for increasing precursor concentration, the pH at which brushite nucleates

decreases.[37,38] The pH affects the solubility and hence the supersaturation of the different phases in the $Ca(OH)_2$-H_3PO_4-H_2O system. The precipitation of CaP consumes, depending on the phase, either PO_4^{3-} or HPO_4^{2-} which leads to a decrease in pH due to:

$$H_2PO_4^- \rightarrow HPO_4^{2-} + H^+ \quad (1)$$

$$HPO_4^{2-} \rightarrow PO_4^{3-} + H^+ \quad (2)$$

An indication of the bioactivity of a biomaterial for bone tissue engineering can be obtained by the formation of bone-like apatite on its surface when it is soaked in simulated body fluid (SBF).[39] Despite the criticism and limitations of this technique[40–42], SBF has been regularly used to indicate the apatite-forming and bone-bonding abilities of biomaterials and is generally accepted as a good initial test for *in vitro* behaviour. In this study it was employed to study the transformation of brushite into HAp within an alginate-brushite composite, not to predict the *in vivo* behaviour of the material.

Our group has previously developed several strategies to mineralise alginate beads with HAp.[14,43]. In this study we investigated the mineralisation of alginate in the pH range of 5 to 7 with the specific aim of creating a bioactive composite material of alginate and brushite with controllable phase and mineral content, where the synthesis and/or material itself is cell-compatible.

2. Materials and Methods

2.1. Chemical reagents

All chemical reagents were purchased from Sigma-Aldrich, Norway unless otherwise is stated. De-ionized water (DIW,with a resistivity of 10-15 MΩcm) was used in all of the experiments.

2.2. Preparation of brushite-seeds

Brushite crystals were synthesised as follows. 500 mL of 0.4 M $Ca(NO_3)_2 \cdot 4H_2O$ and 500 mL of 0.4 M KH_2PO_4 and 26 mM KOH were prepared and bubbled with nitrogen gas. The solutions were mixed and the pH was monitored. The precipitates formed were aged under stirring for 2 h after the changes in pH stopped, before they were filtered and washed with DIW and ethanol. The crystals were dried in room temperature and their size was measured using a Coulter Counter Multisizer 3 (Beckman Coulter).

2.3. Composite beads made by counter-diffusion precipitation

The beads were made similarly to previous methods.[43] Briefly, alginate with a guluronic acid residue fraction of F_G=0.68, corresponding to 68 % (FMC Biopolymer) was dissolved in DI-water to a final concentration of 1.8 wt% containing 0.9 wt% sodium chloride. A mixture of $Na_2HPO_4 \cdot 7H_2O$ and $NaH_2PO_4 \cdot 2H_2O$ was added to a phosphate concentration of 300 mM, where the ratio was decided by the final pH (5 to 7). The solution was stirred for at least 1 h. A gelling solution was made by dissolving calcium chloride in DI-water to give a final concentration of 1 M. Tris(hydroxymethyl)aminomethane (TRIS) or sodium acetate (NaAc) was used to buffer the solution at pH 7, or 6 and 5 respectively. The alginate solution was drawn from a needle with the help of a syringe pump and an electrostatic potential between the needle tip and the gelling bath. The needle diameter was 400 µm and it was electrostatically charged at a potential of 7 kV to ensure a uniform bead diameter of $\sim$ 500 µm.

2.4. Composite beads made by counter-diffusion precipitation with brushite-seeds

For seeded beads, brushite-powder was ground using an agate mortar and pestle to disrupt aggregates formed during the drying process, and mixed with alginate solution (1.8 % alginate, 0.9 % NaCl, 300 mM PO_4^{3-}, pH 5) to a final concentration of 0.1 wt%, 1 wt% and 5 wt% of wet mass. The alginate solution was stirred for at least 1 h to ensure homogeneous mixing. Control beads with no phosphate precursor were made with the same seed concentration. Beads were made using the same technique described previously, however, only gelling bath with 1 M $CaCl_2$, 0.9 wt% NaCl, and 100 mM sodium acetate at pH 5 was used.

2.5. Incubation in SBF

Simulated body fluid (SBF) was made following the instructions given by Kokubo & Takadama.[39] Beads made from 4 mL alginate solution were added into plastic tubes filled with 50 mL SBF-solution and placed at 37^{o}C. Beads containing originally 0.1 wt%, 1 wt% and 5 wt% brushite-seeds were kept in SBF-solution for 24 h, 72 h and 168 h respectively, before they were removed and characterised. Non-mineralised beads without seeds were kept for 168 h in SBF before characterisation as a control.

2.6. Material Characterisation

The beads were optically imaged in the wet state using an inverted microscope (Eclipse TS100, Nikon, Japan).

SEM analysis (Hitachi S-5500 S(T)EM) was performed with an acceleration voltage of 1-10 kV. The sample beads were dehydrated in increasing concentrations of ethanol. The ethanol was then substituted with acetone before they were critical point dried (Emitech K850 critical point dryer). The beads were placed on SEM-stubs with carbon tape and sputter coated (Cressington 208 HR) with a 5-10 nm layer of platinum/palladium (80/20). Chosen beads were cut in the wet state by embedding them in an alginate cylinder, gelled with the *in-situ*-technique[44], or

agarose cylinder, where a 2 % agarose solution was heated on a hot plate and the beads were introduced before the gel had set. These cylinders were cut into 100 or 200 µm sections using a vibrating blade microtome (VT1000S, Leica Biosystems, Nussloch GmBH, Germany). These sections were then dried and mounted using the same procedure as for whole beads.

Powder XRD (D8 Advance DaVinci, Bruker AXS GmBH, Germany) was performed in the range of 5-75^o with a step size of 0.013^o and step time of 0.67 s. Alginate-CaP composites were air-dried and crushed with a mortar and pestle before they were analyzed. Rietveld analysis (Topas4.2, Bruker) was performed in order to assess the relative amount of mineral phases. Background parameters, sample displacement, a scale factor, crystallite size and cell parameters were refined. In order to check the reliability of Rietveld analysis on the samples, analysis on mixes of pure mineral samples with known sample ratios was performed.

Thermogravimetric analysis (TGA) (Netzsch STA449C TGA, Netzsch-Gertebau GmbH, Germany) was performed in the temperature range of 25-1000^{o}C at a heating rate of 20^{o}C min^{-1} under an air flow of 80 mL min^{-1}. A 20 min hold between 70-100^{o}C was performed in order to remove any adsorbed water. In order to estimate the mineral content in the beads the curves describing sample residual mass $m(T)$ were modeled by adding a fraction f of the curve for the pure minerals to a fraction 1-f of the curve for pure alginate where the fraction f denotes the assumed mineral content. For cases where there was more than one mineral phase the relative amount of the minerals, as found with Rietveld analysis, was used:

$$\Delta m(T) = f_H \Delta m_H(T) + f_B \Delta m_B(T) + (1 - f_H - f_B)\Delta m_{Alg}(T) \quad (3)$$

where $\Delta m_H(T)$ and $\Delta m_B(T)$ are the mass loss curve for pure HAp and brushite mineral phases, $\Delta m_{Alg}(T)$ is the mass loss curve for alginate gel, f_H and f_B are the fractions of HAp and brushite. Total mineral fraction ($f_H + f_B$) was then fitted in order for the modelled TGA curves to match the experimental data at at 1000^{o}C. An example of this can be seen in Figure S1 in the supplementary information. The error was calculated based on control samples.

Attenuated total reflection Fourier transform infrared (ATR-FTIR) spectroscopy (Nicolet 8700 ATR-FTIR spectrometer, ThermoFisher Scientific, USA) was performed in the range of 550-4000 cm^{-1} at room temperature. An average of 32 scans was taken.

2.7. Cell experiments

Murine calvarial pre-osteoblast cells, MC3T3-E1 subclone 4 (ATCC® CRL-2593^{TM}) were cultured to 80 % confluency in α-MEM supplemented with 1 µm mL^{-1} gensumycin, 2 mM glutamine and 10 % fetal calf serum, before trypsinising and mixing with alginate at a final concentration of 1 x 10^6 cells mL^{-1}. 300 mM PO_4 and 1 wt% brushite seeds were added to the alginate and the 0.9 % saline was added to give a final alginate concentration of 1.8 wt%. Alginate was also prepared in the same way without phosphate solution or brushite seeds. Microbeads containing cells were produced by electrostatic extrusion as described previously.[43] The gelling solution used as either 300 mM $CaCl_2$ or 1 M $CaCl_2$ containing 0.9 % NaCl and adjusted to pH 5 with 50 mM or 100 mM NaAc respectively, or 50 mM $CaCl_2$ for non-mineralised control samples containing no phosphate or brushite seeds. 10 mL alginate microbeads were left in the gelling solution for 10 minutes prior to washing with PBS and then culture media and suspending in 10 mL culture media and placing in an incubator. To assess cell viability post encapsulation a combination of a calcein-AM / ethidium homodimer-1 assay (LIVE/DEAD® Viability/Cytotoxicity Kit, L-3224, Molecular Probes®) and an AlamarBlue® viability assay (DAL1100, Molecular Probes®) were used. This combination of assays was used because of difficulties in accurately counting cells stained using the LIVE/DEAD assay in mineralised samples, which were much more optically dense than non-mineralised controls. The AlamarBlue assay relies on optical measurements of the incubating media and is therefore not influenced by the optical properties of the samples. Viability was monitored at 1, 3, 10 and 15 days post encapsulation on 6 repeat samples of known mass (between 0.4 - 0.6 g). At each time point the live/dead cell count in non-mineralised control samples was taken and AlamarBlue reduction was measured for all samples (optical absorption at 570 and 590 nm, Perkin Elmer Victor 3). Comparing the results obtained by the AlamarBlue reduction assay allowed the % viability of experimental samples to be normalised to the viability of non-mineralised control samples measured by the live/dead assay. The viability of the control sample has been normalized with respect to the total amount of encapsulated cells at the start of the experiment.

3. Results and Discussion

3.1. Investigating parameters for CaP precipitation within alginate microbeads

Alginate/CaP composite beads were prepared by the counter diffusion method, as described in section 2.3. This arrangement created a highly dynamic system in which phosphate ions diffused out of the bead, Ca^{2+} diffused into the bead, and gelling of the alginate and precipitation of CaP happened simultaneously. The formation of mineral consumed phosphate ions which lowered the pH locally in the hydrogel, as can be seen from Equations (1) and (2). As a result, a local pH-gradient within the alginate beads was formed, and the pH in the gelling bath decreased over time, see Figure 1. Both the gelling and the mineral precipitation processes consumed calcium ions.

In the first instance, we have investigated an approach to produce alginate/brushite composites similar to that

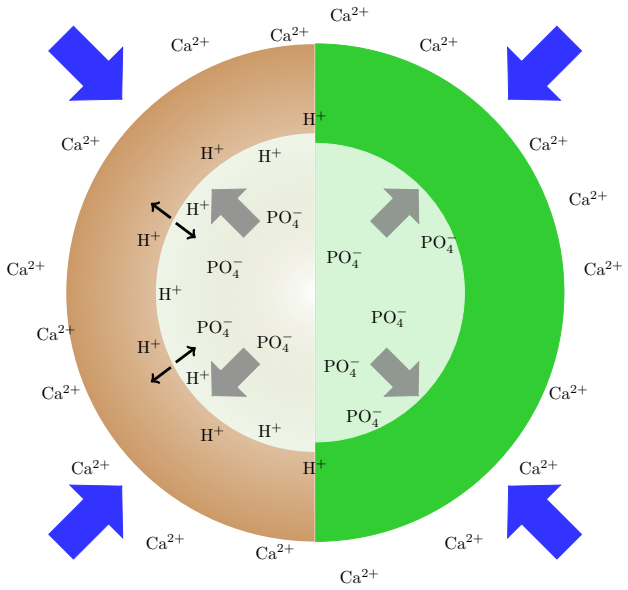

Figure 1 A schematic illustrating the gelling and mineralising system. After the drop has entered the gelling bath, Ca^{2+} diffuses inwards (blue arrows), phosphate ions (PO_4^-) diffuses outwards (gray arrows), gelling and mineralising occurs at the front of Ca^{2+} diffusion illustrated by a color difference in the figure. On the right, the green color indicates gelled alginate. On the left, the brown color illustrates mineral formation and the assosciated local release of H^+, their diffusion indicated by black arrows. The mineral front is trailing slightly behind the gelling front.

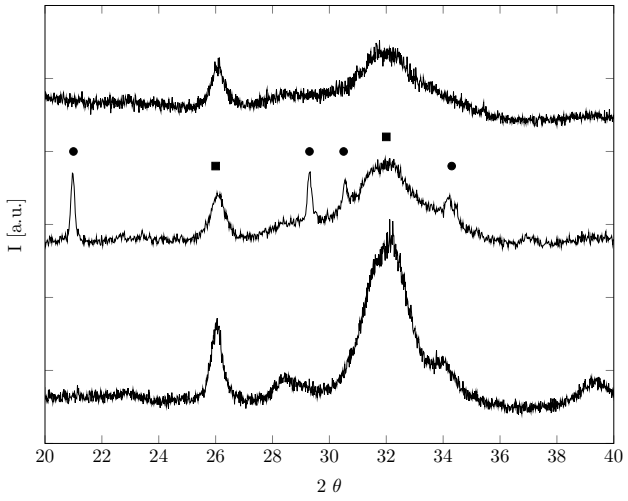

Figure 2 XRD-spectra for samples made with 300 mM phosphate in the alginate solution and 1 M calcium chloride in the gelling bath. **Bottom:** No buffer. **Middle:** A representative sample from the pH-study with 50 mM NaAc buffer. **Top:** A sample with 500 mM NaAc buffer. • denotes brushite, ■ denotes HAp.

proposed by Amer *et al.*[32], although with reversed Ca/P ratio and a smaller bead size. The reversed Ca/P ratio was needed to form stable alginate gels[43]. This is due to the fact that the affinity between phosphate ions and calcium ions is larger then that between alginate and calcium ions. Consequently, if the calcium concentration in the gelling bath is too low, the available Ca-ions are consumed by the forming mineral phase and a stable alginate gel is not formed.

Surprisingly, no evidence of monetite or brushite was found within the hydrogel network. Contrary to the their observations, the mineral phase within the beads produced in this study was poorly crystalline HAp, as seen in the lower spectrum of Figure 2. An optical image of a representative sample can be seen in Figure 3 A. It was also observed that some of the phosphate precursor diffused out of the beads and formed brushite-precipitates in the gelling bath. It is not only the Ca/P ratio that plays a role in formation of CaP-precipitates, the pH is a determining factor for nucleation of the different phases.[24] Unfortunately, no information about pH is given in the work of Amer *et al.* In this work, the pH in the gelling bath was observed to change from an initial value of pH = 7 to as low as pH = 3 during bead formation. This large drop in pH can also contribute in destabilising the gel. The pK_a of alginate ranges from 3.4 to 4.4 depending on the type of alginate and the conditions.[45] At such low pH alginate can begin to lose its charge and hence affinity for Ca^{2+}. This effect in combination with the consumption of Ca^{2+} due to mineral formation can lead to destabilisation the gel bead, seen as wrinkles in Figure 3 B. Similar observations have been reported earlier, however, charge-neutralisation was then due to an oppositely charged polymer, not pH.[46]

In order to investigate the role of pH, on both nucleation and growth of different CaP crystal phases, a series of experiments was performed where the initial pH in both the alginate solution and the gelling bath was systematically varied between pH = 5 and pH = 7 (a total of 9 combinations) by the addition of a buffer (see Materials and Methods). For a sample formed using 50 mM buffer, upon inspection with optical microscopy (Figure 3 B), it was clear that the mineralisation was inhomogeneous in the sense that individual beads were mineralised differently. This sample was representative for most of the experiments. Note that this buffer concentration was not sufficient to keep the pH stable during bead formation. This time-dependent change in the pH-value was believed to be the cause of the inhomogeneity observed in Figure 3. XRD-results showed that the mineral formed was, in most cases, not pure phase, but a mixture of brushite and HAp, as can be seen in the top spectrum of Figure 2, and in some cases minor amounts of OCP. The estimated amount of mineral for the different samples varied between 2-49 $\pm$3 weight percent of dry mass, corresponding to 0.1-1.8 $\pm$0.2 weight percent mineral content in the hydrated gel.

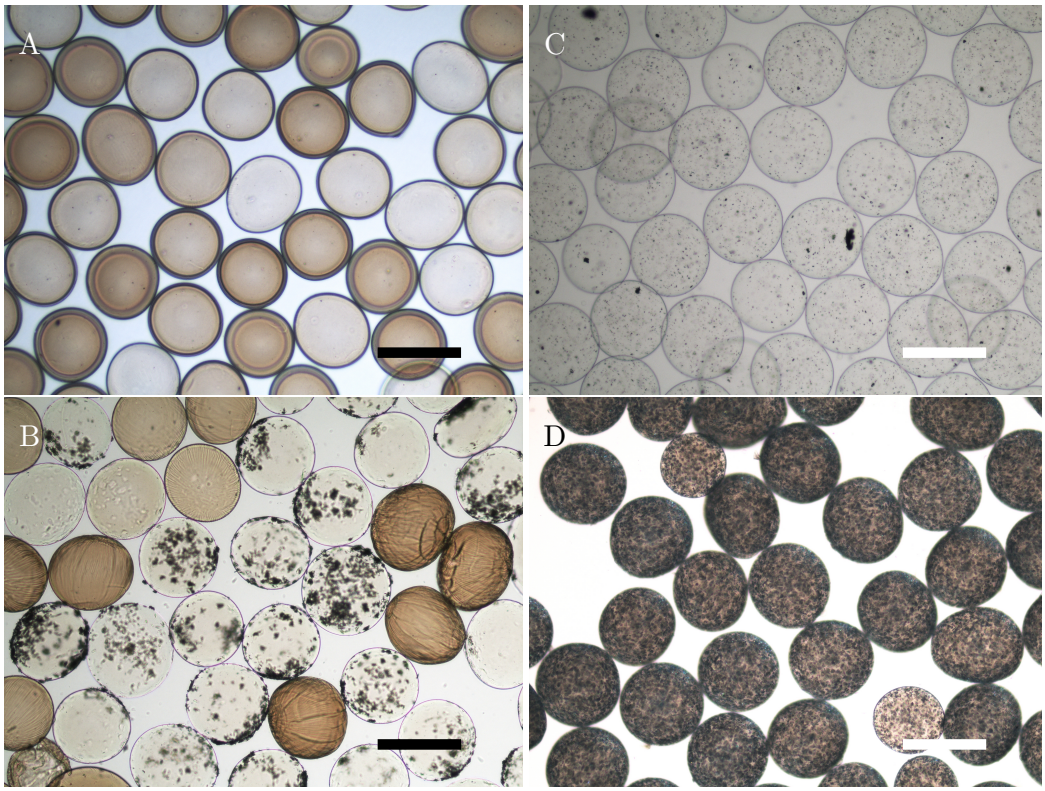

Figure 3 Optical images of **A:** A sample gelled in an unbuffered bath. **B:**A sample made with alginate solution at pH 7 and gelling bath at pH 6 with 50 mM NaAc buffer. Brown beads are mineralised throughout, while black spots are larger brushite-crystals on the surface of the beads. **C:** A sample with 0.1 % brushite-seeds without phosphate precursor. **D:** A sample with 0.1 % brushite-seeds with phosphate precursor and gelling bath at pH 5 with 100 mM NaAc buffer. Scale bars are 500 µm.

The buffer strength was increased to 100 and 500 mM in an attempt to stabilize the pH at pH = 5. In both cases the change in pH was as expected lower, however, these experiments resulted in pure phase HAp within the alginate-composite as can be seen in Figure 2 for a sample with 500 mM buffer. A possible explanation for this is that the ideal pH for formation of brushite is somewhere below pH = 5, however, if the pH within the microbead is too low, the phosphate precursor might diffuse out of the alginate network before any mineral is formed. Hence, at no buffering HAp is formed initially and the pH drops quickly to a value where no new crystals are nucleated. For strong buffering the pH does not drop into the region where brushite formation is favored. The lower concentration of buffer (50 mM) allowed for the formation of some brushite, but the process was poorly controlled. For the further experiments an initial pH = 5 in the gelling bath was chosen as a compromise between brushite-formation and cell survival. The buffer concentration was also increased to 100 mM in order to ensure more stable conditions over time in the gelling bath.

The variation in mineral amount and occurrence of several phases indicated a complex crystallisation process within the alginate microbeads, sensitive to the local supersaturation, pH, precursor concentration, and precursor ratios, all of which were changing during bead formation. A lack of control over the process was identified, as the resulting mineral phase and amount varied between experiments performed under the same conditions. However, a clear trend from these experiments was that a lower pH in the alginate solution lead to a lower amount of mineral within the hydrogel beads, regardless of the initial pH in the gelling bath. A possible explanation for this is that the higher local pH within the gel network, immediately after the droplet entered the gelling bath, affected the local supersaturation and allowed for faster nucleation of mineral. In cases where the initial pH within the beads were lower, more of the phosphate precursor diffused out into the gelling bath before precipitation occurred. The high initial pH is incompatible with the formation of brushite, at least in a controlled manner. To overcome this, brushite seed crystals were incorporated in the alginate solution in order to promote early growth of brushite and gain control over which phases nucleate in the sample.

3.2. Control of brushite formation within alginate matrix in using seed crystals

To promote the growth of brushite within the alginate network, brushite seeds were introduced into the alginate

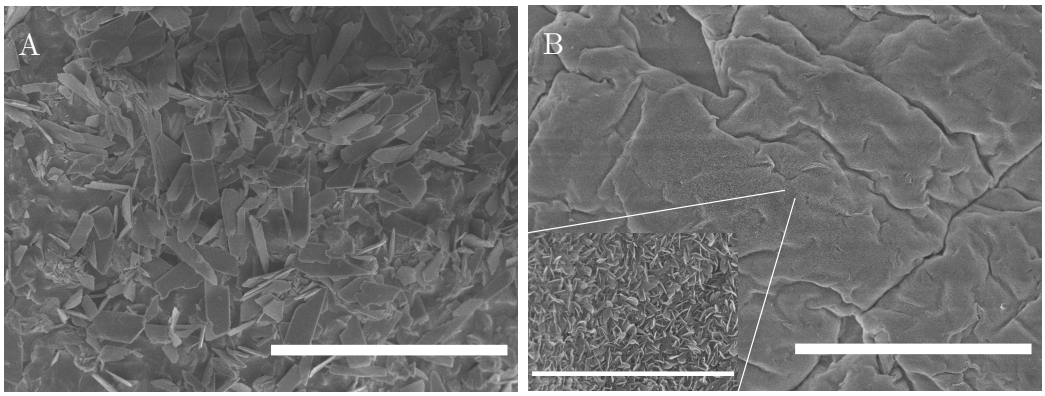

Figure 4 SEM micrograph of the surface an alginate microbead made with medium seed concentration and phosphate precursor. **A:** before and **B:** after 168 h in SBF. Scale bars are 30 μm and 2 μm for the inset.

Table 1 The results for seeded beads gelled in 1 M $CaCl_2$, 0.9 wt% NaCl, 100 mM NaAc. The mass percentage refers to mineral content while the last column refers to the brushite-percentage of this mineral.

Seed conc.	PO_4 mM	Final pH	Dry mass %	Wet mass %	Brushite %
0.1 %	300	4.88	71 ± 3	4.5 ± 0.6	95
0.1 %	0	5.00	0 ± 3	0.0 ± 0.1	100
1 %	300	4.85	79 ± 3	6.9 ± 1.2	99
1 %	0	5.00	32 ± 3	0.8 ± 0.2	100
5 %	300	4.73	85 ± 3	10.6 ± 2.5	98
5 %	0	5.00	72 ± 3	4.7 ± 0.5	100

solution at three different concentrations: 0.1, 1 and 5 weight percent (hereby referred to as low, medium and high concentration of seeds). Seed crystals had a size range of approximately 30 μm, measured by Coulter counter. Dried seeds were grounded using a mortar and pestle priory to mixing with the alginate solution to distribute the seeds evenly and avoid clogging of the needle. Phase purity of the seeds were verified with XRD. Beads were then made with alginate solutions containing seeds and the phosphate precursor. The pH of the gelling bath was kept at pH 5 with 100 mM sodium acetate buffer and contained 1 M $CaCl_2$ and 0.9 % NaCl.

Table 1 summarizes results obtained for the seeded experiments at conditions described above. All samples, made with phosphate precursor and brushite-seeds, contained close to pure phase brushite with 71 ± 3 to 86 ± 3 percent mineral amount (dry mass) corresponding to 4.5 ± 0.6 to 10.6 ± 2.5 percent wet mass. Figure 3 C and D shows optical images of low concentration seeded beads without and with phosphate precursor. Comparing Figure 3 A and B to Figure 3 D, the mineralisation of the beads was clearly more homogeneous when seed-crystals were incorporated in the alginate solution. As can be seen from Table 1, there was an increase in mineral content from the seeded control sample without phosphate precursor to the beads with seeds and phosphate precursor. Calculations based on TGA-data indicated that similar amounts of new mineral was formed in all samples. The increase can either arise from growth of the seeds, nucleation of new crystals or a combination of these.

Optical microscopy indicated the formation of new mineral crystals as can be seen when comparing Figure 3 C to D. This was confirmed by SEM-images of the surface and cross-sections. Figure 4 A shows the surface of a medium concentration seeded bead. A large number of crystals can be observed on the surface, which were not observed for beads with brushite-seeds, but without phosphate precursor (Figure S2 supplementary info). SEM images from the cross-section of a low concentration seeded bead (Figure 5) clearly show mineral crystals (white arrows) situated within the alginate network. These are much smaller in size than the seed crystals which suggests that they were nucleated during bead fabrication.

Although the mineralisation was homogeneous between beads, the mineral distribution inside the alginate network was not homogeneous. Mineral formed a denser shell on the outside, and the beads appeared less mineralised towards the center. This was as expected from previous work with the counter-diffusion method at high supersaturation.[14] The difference in mineral content can be seen in Figure 5, where images from the center and the edge of a cross-section from a bead is shown. There is also an image (Figure 5 C) of a seed crystal showing the difference in size between seeded crystals and nucleated crystals. Note the difference in size of the seed crystal and surface crystals compared to the crystals within the network (Figure 4 A vs Figure 5 A). The smaller crystals within the network suggested a different growth rate than for the crystals on the surface.

To assess the quality of the XRD analysis, control experiments were performed. Three samples of 33.3 % brushite and 66.7 % HAp were made individually and characterized. Rietveld analysis resulted in 38.8 ± 0.7 % brushite. For a series of 6 mixtures ranging from 0

to 100 % brushite, the analysis consistently overestimated the amount of brushite by 3.2 ± 2.4 percentage points. These results indicate that the analysis had good precision, albeit with a systematic overestimation. One should note a large increase in the brushite signal between the control and 0 h sample in the XRD spectra shown in Figure 6. The control sample contained only seeds (0.1 %) and no mineral precursor while the 0 h sample was mineralized with 300 mM phosphate. There was a large increase in the brushite signal, indicating growth or formation of new brushite crystals within the sample (also seen in Figure 3D), at the same time no peaks associated with HAp phase were present. These peaks appeared only after storage. From control samples of pure HAp and brushite crystals mixed at a known ratio, the HAp peaks were easily detectable in a mix with 20 % HAp and 80 % brushite (data not shown). This indicates that a minimal amount HAp was formed initially.

For TGA-modeling, low, medium and high concentration of seeds, corresponding to dry mass percent of 5.3, 35.7 and 73.5, assuming only alginate and CaP remains after drying, were introduced into an alginate solution without phosphate precursor. TGA of these samples resulted in a calculated dry mass percent of 0 ± 3, 32 ± 3 and 72 ± 3. The expected ideal values are outside the uncertainties of the calculated values for the lower seed concentrations, however they show a similar increase in mass as would be expected, suggesting that the method is reliable although somewhat inaccurate. For the pure alginate control there was a pronounced weight loss from 650-800^{o}C related to the decomposition of calcium carbonate into calcium oxide. This behaviour was not observed when phosphate mineral was precipitated during gelling (see Figure S1 and a short discussion given in the Supplementary Info). Due to this change in decomposition behaviour and the overestimation of brushite from the Rietveld analysis, the TGA-model overestimated the mineral content by about 5 percentage points dry mass for heavily mineralised samples. The values presented in Figure 7 are midpoints between the original model and a model with 3 % less brushite and 5 percentage points less estimated dry mass, with error bars reaching the two extremes.

The seeds introduced into the alginate solution affected the crystallisation conditions for the whole bead, not just in immediate proximity of the seeds. As can be seen from Figure 5, new crystals of brushite were nucleated within the alginate network. This could either result from a change in the conditions of the alginate solution, where a combination of pH and supersaturation favored the nucleation of brushite or it may have been a secondary nucleation mechanism.[47] Nucleation occurs much more readily when solute crystals are already present in the medium due to lowered energy barrier where parent crystals act as catalysts for nucleation.[48]

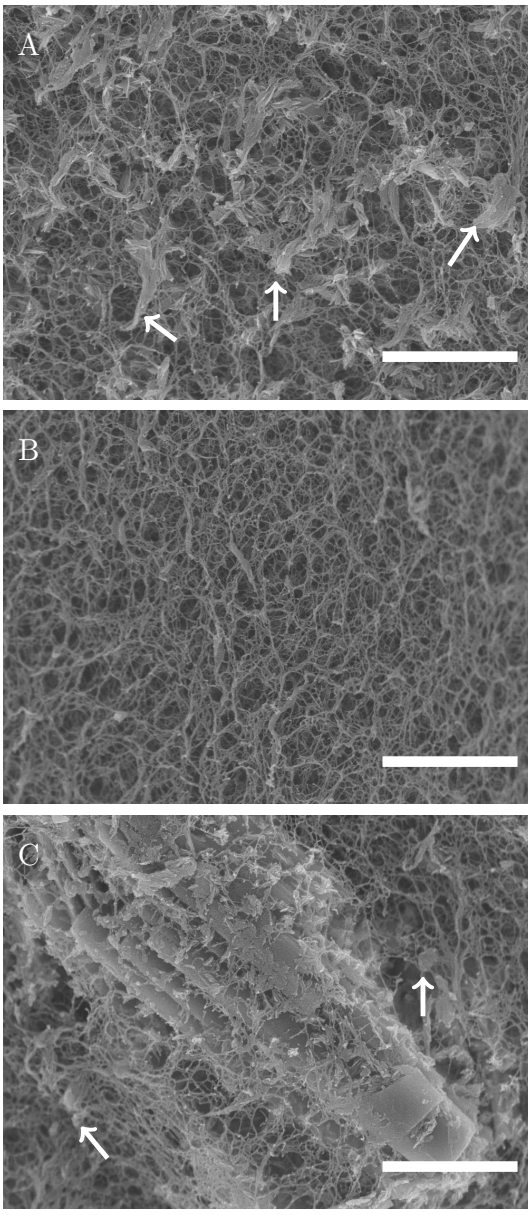

Figure 5 SEM micrographs of the cross-section of a low concentration seeded bead. **A**: mineralised network in the outer region, **B**: less mineralised network towards the center, and **C**: the surroundings of a brushite-seed. White arrows indicate selected mineral crystals. Scalebar is 1 µm

3.3. Bioactivity of alginate composites in SBF

In order to evaluate the potential bioactivity of these CaP mineral-alginate composite materials, samples were incubated in SBF for 24, 72 and 168 h before they were characterized. Figure 6 shows the XRD-results for the low seed concentration sample. The results clearly show a gradual increase of HAp and decrease of brushite signal which was observed for all the different seed concentrations. This data is summarized in Figure 7, where a clear transformation of initial brushite into HAp

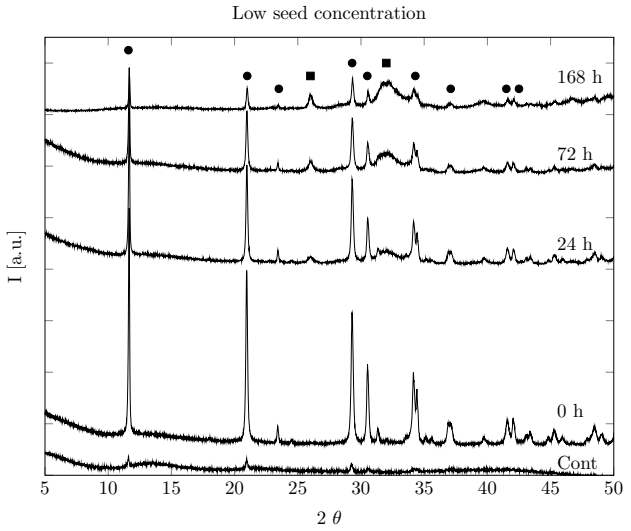

Figure 6 XRD-spectra for the different timepoints for a sample with low concentration brushite-seeds with PO_4^{3-}. • denotes brushite, ■ denotes HAp. The legend numbers indicate number of hours in SBF and the control sample did not contain PO_4^{3-}-precursor.

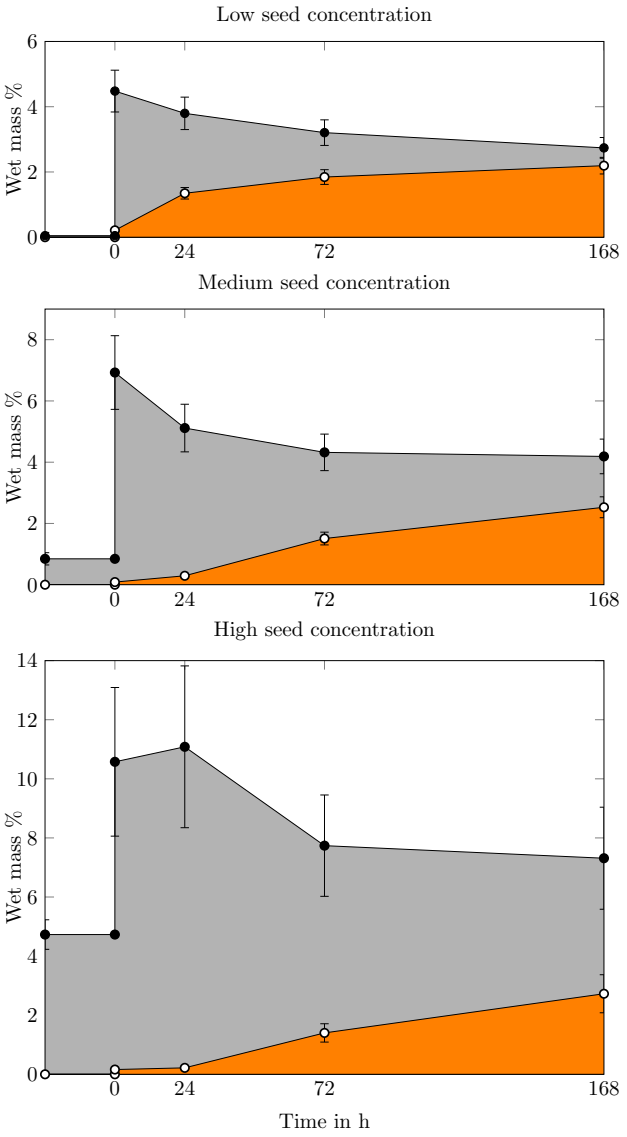

Figure 7 Graphs of the mineral evolution for the three different sample groups as estimated by XRD and TGA (Eq. (3)). Black points: Total mineral content. White points and orange area: HAp content. Grey area: brushite content. The area before the 0 h point shows the amount of mineral introduced as seeds. The y-axis is scaled so the figures are directly comparable.

is observed over time. An initial decrease in total mineral content can also be seen. The image in Figure 4 A was taken before incubation in SBF, and the one in B was taken after 168 h incubation in SBF. For the composite containing phosphate precursor there was, before incubation, a large number of brushite crystals on the surface. These appear to have dissolved and reprecipitated as smaller HAp-crystals, seen in the inset in Figure 4 B. This dissolution is presumably the cause of the decrease in the overall mineral content. These results also show that the lowest seed concentration transformed into HAp earlier than the other samples. As controls, alginate beads with seeds, but no phosphate precursor and alginate beads without seeds or phosphate precursor were also kept in SBF for 168 h. The seeded control showed no conversion into HAp (see Figure S2 in Supplementary Info), while the pure alginate control showed no mineral formation.

This study was performed under static conditions and was therefore not a prediction of actual *in vivo* behaviour.[49] This was done in order to study the transformation behavior of the mineral in a solution supersaturated with respect to HAp. The dissolution of brushite and formation of HAp occured under the same initial conditions in the different sample groups. Comparing these results to the work of Miller *et al.*[50], who performed a study of brushite-transformation in 4 different SBF-solution, including a TRIS-buffered solution similiar to the one used in this study, the behavior is similar except for two main points. In this study, the initial brushite has not been completely dissolved or transformed within 168 h. That is probably due to the fact that static conditions were used. A more interesting observation is that no OCP was observed in this work. This can be seen in Figure 6 where two distinct peaks of OCP (9.45^o and 9.77^o) are absent.

FTIR-analysis, shown in Figure 8, confirmed the formation of brushite for all samples seeded with brushite, with strong absorbance bands at 986 and 1005 cm^{-1} corresponding to the $\upsilon 2$ P-O symmetrical stretching mode and 1059, 1125 and 1137 cm^{-1} corresponding to the $\upsilon 6$ triply degenerated P-O stretching mode.[51] Changes in the FTIR spectrum occurred for all samples exposed to SBF, which indicated a change from HPO_4^{2-} to PO_4^{3-}. This can be seen in the disappearance of the $\upsilon 3$ P-O(H) stretching mode at 875 cm^{-1} and the appearance of a

strong adsorption at 1025 cm^{-1}. Also changes occurred in the $\upsilon 4$ O-P-O(H) bending mode, which is located at 578 cm^{-1} for brushite and 602 cm^{-1} for HAp.[51,52] These changes occurred more rapidly for samples formed with less initial seed material. After 168 h incubation, low concentration seeded composites had almost completely lost the vibrational modes associated with brushite and the resulting spectra resembled poorly crystalline HA; by comparison high concentration seeded samples, however, had only partially converted by this time.

FTIR-results largely reflect what was found by XRD-analysis, shown in Figure 6, however the loss of intensity of the brushite-signal appears earlier for FTIR. This could suggest a loss of protons and formation of an intermediate amorphous phase, before reprecipitation to HAp. As XRD-techniques rely on crystalline samples for signal, amorphous phases would not be detected by XRD.

The accelerated transformation of brushite into HAp at decreased seed concentration may derive from the smaller size of the newly formed brushite crystals. For higher seed concentrations, a higher amount of the initial phosphate will be consumed in the crystal growth of these seeds. In the cases of higher seed loading, consumption of ions by growth would likely have caused a decrease in number of newly formed particles.[48] The smaller crystals had a higher surface area and therefore dissolved more readily. The increased bioactivity of smaller crystals is further corroborated by a control sample in which beads containing medium seed concentration without phosphate precursor showed no conversion into HAp after 168 h in SBF-solution.

3.4. Cell encapsulation and survival

Alginate hydrogels provide a good matrix for cell encapsulation, we have previously shown that cells can also be encapsulated and survive in alginate microbeads mineralised with HAp.[53,54] Gryshkov *et al.* has also shown that the high voltage does not affect cell viabilitiy[55]. Previously, the mineralised alginate was synthesised under mild conditions of mineral precursor concentrations and near physiological pH. Here we have used more acidic conditions to achieve the desired brushite mineral phase. Since cells may not survive such low pH, we tested the viability of pre-osteoblast cells post encapsulation. Cells were encapsulated in alginate containing 1 % brushite seeds, 300 mM PO_4 and gelled in 1 M $CaCl_2$ and 100 mM NaAc at pH 5 or 300 mM $CaCl_2$ and 50 mM NaAc and compared to non-mineralised control beads made with pure alginate and gelled in 50 mM $CaCl_2$. Surprisingly there was little difference in cell viability 24 h after encapsulation between controls and mineralised beads gelled in 300 mM $CaCl_2$ (87.2 $\pm$ 6.0 % vs 88.3 $\pm$ 6.2 %). However, a lower viability for mineralised samples gelled in 1 M $CaCl_2$ was recorded (79.4 $\pm$ 6.7 %). Cell viability reduced gradually over the 15 days of the culture period for all samples. After

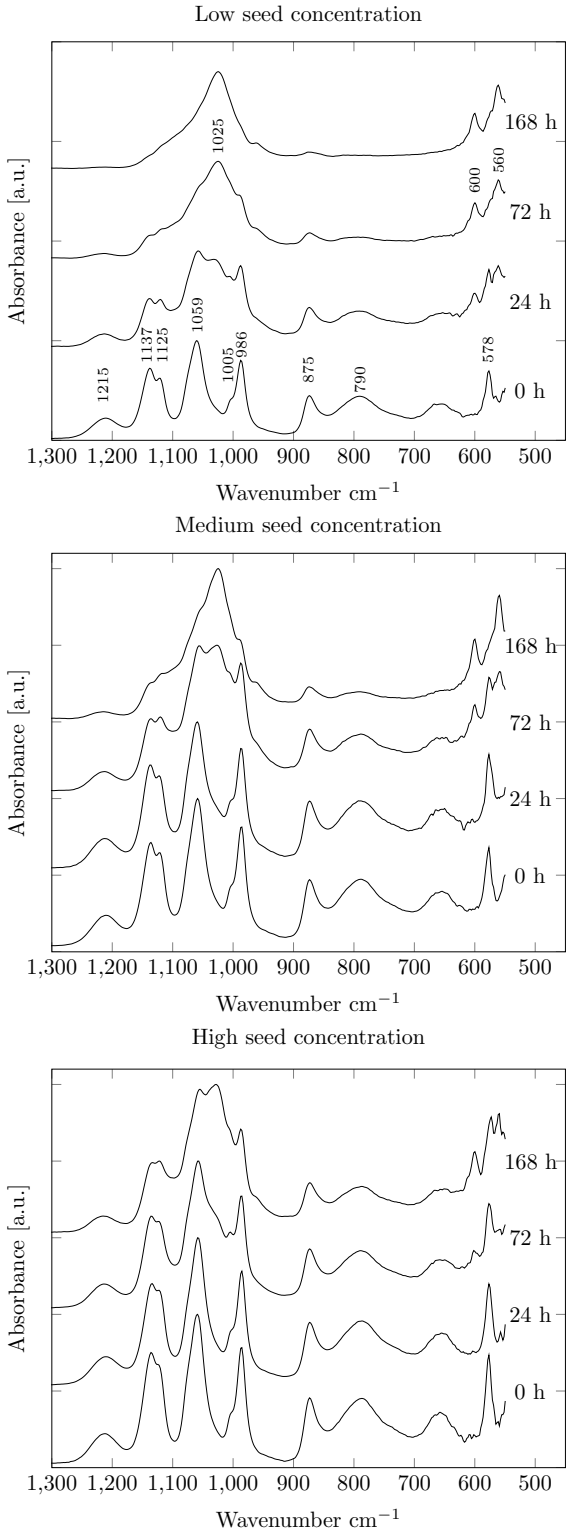

Figure 8 FTIR-spectra of the different samples with 0.1 %, 1 % and 5 % seed concentrations.

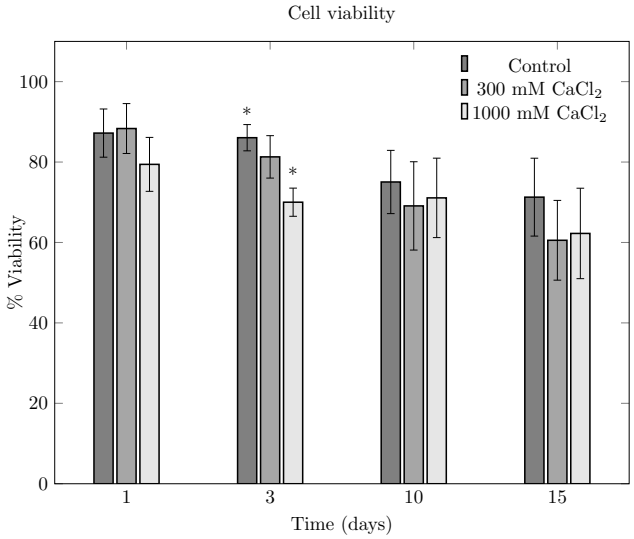

Figure 9 The cell viability in % at four different timepoints for two different calcium concentrations compared to a non-mineralised control. The buffer concentrations were 50 mM NaAc for the control and 300 mM $CaCl_2$ sample and 100 mM NaAc for the 1000 mM $CaCl_2$ sample. The * marks statistical significance ($p<0.01$).

15 days of culture cell viability was 60.5 ± 9.9 % and 62.2 ± 11.2 % for mineralised samples and 71.2 ± 9.7 % for non mineralised controls. This gradual reduction was probably due to natural cell death without renewal since the cells appeared to not divide within the alginate matrix as very similar numbers of cells were observed within each bead at each time point. Since the rate of cell death was very similar for all samples it would appear that the mineral made in either condition had little influence on cell viability.

4. Conclusions

Building upon our previous work regarding counter-diffusion synthesis of alginate-calcium phosphate (HAp) composite materials, here we have formulated robust methods to control the phase purity and amount of brushite formed within alginate hydrogels. These new materials may have a significant advantage over HAp containing alginates as bone tissue engineering constructs, since brushite is metastable under physiological conditions and will convert to HAp, as we have demonstrated in simulated body fluid, and may act as a reservoir for essential ions for bone remodelling. Reliable nucleation of the preferred brushite phase inside the alginate network proved more complicated than in aqueous solution in the absence of alginate, where control over the initial parameters of pH and stoichiometry was enough to predict the resulting phase. The incorporation of brushite seed crystals to the alginate solution prior to gelation resulted in improved control and reproducibility of the mineral phase and by adjusting the amount of seeds and precursor concentration, the amount of mineral could also be tuned. The bioactivity of the precipitated mineral was shown to be higher than that of mixtures of preformed mineral incorporated in an alginate matrix, likely due to the smaller crystal size of mineral precipitated within the alginate matrix. Furthermore, we found that our synthesis method was well tolerated by pre-osteoblast cells, and cell viability was similar to non-mineralised control samples post encapsulation and survived well over a period of 15 days. This is significant for the intended use of these materials as support structures for cells in the context of bone tissue regeneration.

5. Acknowledgements

We acknowledge the Research Council of Norway for financial support (FRINATEK project 214607). We thank Dr. O. Sigurjonsson, Reykjavik University, Iceland for the donation of cells used in this study. We also thank Dr. Berit L. Strand for fruitful advice regarding alginate.

References

[1] Hollister S J 2009 *Advanced Materials* **21** 3330–42 ISSN 1521-4095 URL http://www.ncbi.nlm.nih.gov/pubmed/20882500

[2] Rokstad A M A, Lacík I, de Vos P and Strand B L 2014 *Advanced drug delivery reviews* **67-68** 111–30 ISSN 1872-8294 URL http://www.sciencedirect.com/science/article/pii/S0169409X13001646

[3] Place E S, Evans N D and Stevens M M 2009 *Nature materials* **8** 457–70 ISSN 1476-1122 URL http://www.ncbi.nlm.nih.gov/pubmed/19458646

[4] Hoffman A S 2002 *Advanced Drug Delivery Reviews* **54** 3–12 ISSN 0169409X URL http://www.sciencedirect.com/science/article/pii/S0169409X01002393

[5] Dragan E S 2014 *Chemical Engineering Journal* **243** 572–590 ISSN 13858947 URL http://www.sciencedirect.com/science/article/pii/S1385894714000904

[6] Amini A R, Laurencin C T and Nukavarapu S P 2012 *Critical Reviews in Biomedical Engineering* **40** 363–408 ISSN 0278-940X URL http://www.dl.begellhouse.com/journals/4b27cbfc562e21b8,489cce62273b4868,20e3cde6200d53aa.html

[7] Drury J L and Mooney D J 2003 *Biomaterials* **24** 4337–4351 ISSN 01429612 URL http://linkinghub.elsevier.com/retrieve/pii/S0142961203003405

[8] Kolambkar Y M, Dupont K M, Boerckel J D, Huebsch N, Mooney D J, Hutmacher D W and Guldberg R E 2011 *Biomaterials* **32** 65–74 ISSN 1878-5905 URL http://www.sciencedirect.com/science/article/pii/S0142961210011129

[9] Cohen J 1998 *The Journal of bone and joint surgery. American volume* **80** 1554 ISSN 0021-9355

[10] Rho J Y, Kuhn-Spearing L and Zioupos P 1998 *Medical engineering & physics* **20** 92–102 ISSN 1350-4533 URL http://www.ncbi.nlm.nih.gov/pubmed/21885114

[11] Bernhardt A, Despang F, Lode A, Demmler A, Hanke T and Gelinsky M 2009 *Journal of Tissue Engineering and Regenerative Medicine* **3** 54–62 URL http://onlinelibrary.wiley.com/doi/10.1002/term.134/abstract

[12] Yokoi T, Kawashita M, Kikuta K and Ohtsuki C 2010 *Journal of Crystal Growth* **312** 2376–2382 ISSN 00220248 URL http://www.sciencedirect.com/science/article/pii/S0022024810003544

[13] Rajkumar M, Meenakshisundaram N and Rajendran V 2011 *Materials Characterization* **62** 469–479 ISSN 10445803 URL http://www.sciencedirect.com/science/article/pii/S1044580311000489http://linkinghub.elsevier.com/retrieve/pii/S1044580311000489

[14] Xie M, Olderoy M O, Zhang Z, Andreassen J P, Strand B L and Sikorski P 2012 *RSC Advances* **2** 1457–1465 URL http://dx.doi.org/10.1039/C1RA00750E

[15] Li Z, Su Y, Xie B, Wang H, Wen T, He C, Shen H, Wu D and Wang D 2013 *Journal of Materials Chemistry B* **1** 1755 ISSN 2050-750X URL http://pubs.rsc.org/en/content/articlehtml/2013/tb/c3tb00246bhttp://xlink.rsc.org/?DOI=c3tb00246b

[16] Luo Y, Lode A, Sonntag F, Nies B and Gelinsky M 2013 *Journal of Materials Chemistry B* **1** 4088 ISSN 2050-750X URL http://xlink.rsc.org/?DOI=c3tb20511h

[17] Zhu C, Bao G and Wang N 2000 *Annual review of biomedical engineering* **2** 189–226 ISSN 1523-9829 URL http://www.annualreviews.org/doi/full/10.1146/annurev.bioeng.2.1.189?url_ver=Z39.88-2003&rfr_id=ori:rid:crossref.org&rfr_dat=cr_pub=pubmed

[18] Suárez-González D, Barnhart K, Saito E, Vanderby R, Hollister S J and Murphy W L 2010 *Journal of biomedical materials research. Part A* **95** 222–34 ISSN 1552-4965 URL http://www.pubmedcentral.nih.gov/articlerender.fcgi?artid=2928845&tool=pmcentrez&rendertype=abstract

[19] Lin H R and Yeh Y J 2004 *J Biomed Mater Res B Appl Biomater.* **71** 52–65 ISSN 1552-4973 URL http://www.ncbi.nlm.nih.gov/pubmed/15368228

[20] Albrektsson T and Johansson C 2001 *Eur Spine J.* **10 Suppl 2** S96–101 ISSN 0940-6719 URL http://www.pubmedcentral.nih.gov/articlerender.fcgi?artid=3611551&tool=pmcentrez&rendertype=abstract

[21] Johnsson M S and Nancollas G H 1992 *Critical Reviews in Oral Biology & Medicine* **3** 61–82 URL http://cro.sagepub.com/content/3/1/61.abstract

[22] Mirtchi A, Lemaître J and Munting E 1989 *Biomaterials* **10** 634–8 ISSN 0142-9612 URL http://www.ncbi.nlm.nih.gov/pubmed/2611315

[23] Tamimi F, Sheikh Z and Barralet J 2012 *Acta biomaterialia* **8** 474–87 ISSN 1878-7568 URL http://dx.doi.org/10.1016/j.actbio.2011.08.005http://www.ncbi.nlm.nih.gov/pubmed/21856456

[24] Elliott J 1994 *Structure and Chemistry of the Apatites and Other Calcium Orthophosphates* (Elsevier B.V.) ISBN 9780444815828

[25] Apelt D, Theiss F, El-Warrak A, Zlinszky K, Bettschart-Wolfisberger R, Bohner M, Matter S, Auer J and von Rechenberg B 2004 *Biomaterials* **25** 1439–1451 ISSN 01429612 URL http://www.sciencedirect.com/science/article/pii/S014296120300677X

[26] Klammert U, Ignatius A, Wolfram U, Reuther T and Gbureck U 2011 *Acta Biomaterialia* **7** 3469–3475 ISSN 17427061 URL http://linkinghub.elsevier.com/retrieve/pii/S1742706111002236

[27] Kanter B, Geffers M, Ignatius A and Gbureck U 2014 *Acta Biomaterialia* **10** 3279–3287 ISSN 17427061 URL http://linkinghub.elsevier.com/retrieve/pii/S1742706114001883

[28] Habibovic P, Gbureck U, Doillon C, Bassett D, Vanblitterswijk C and Barralet J 2008 *Biomaterials* **29** 944–953 ISSN 01429612 URL http://linkinghub.elsevier.com/retrieve/pii/S0142961207008289

[29] Gbureck U, Hölzel T, Klammert U, Würzler K, Müller F a and Barralet J E 2007 *Advanced Functional Materials* **17** 3940–3945 ISSN 1616301X URL http://doi.wiley.com/10.1002/adfm.200700019

[30] Nanzyo M, Shibata Y and Wada N 2002 *Soil Science and Plant Nutrition* **48** 847–853 ISSN 0038-0768 URL http://dx.doi.org/10.1080/00380768.2002.10408711

[31] Koburger S, Bannerman A, Grover L M, Müller F A, Bowen J and Paxton J Z 2014 *Biomaterials Science* **2** 41 ISSN 2047-4830 URL http://pubs.rsc.org/en/content/articlehtml/2014/bm/c3bm60102ahttp://xlink.rsc.org/?DOI=c3bm60102a

[32] Amer W, Abdelouahdi K, Ramananarivo H R, Fihri A, El Achaby M, Zahouily M, Barakat A, Djessas K, Clark J and Solhy A 2014 *Mater Sci Eng C Mater Biol Appl.* **35** 341–6 ISSN 1873-0191 URL http://www.ncbi.nlm.nih.gov/pubmed/24411386

[33] Kelton K 1991 *Solid State Physics* **45** 75–177 ISSN 00811947 URL http://www.sciencedirect.com/science/article/pii/S0081194708601447

[34] Kashchiev D and van Rosmalen G M 2003 *Crystal Research and Technology* **38** 555–574 ISSN 02321300 URL http://doi.wiley.com/10.1002/crat.200310070

[35] Boistelle R and Lopez-Valero I 1990 *Journal of Crystal Growth* **102** 609–617 ISSN 00220248 URL http://www.sciencedirect.com/science/article/pii/002202489090420P

[36] Wuthier R E, Rice I G S, Wallace J E B, Weaver R L, Legeros R Z and Eanes E D 1985 *Calcif Tissue Int* **37** 401–410

[37] Abbona F, Madsen H and Boistelle R 1986 *Journal of Crystal Growth* **74** 581–590 ISSN 00220248 URL http://linkinghub.elsevier.com/retrieve/pii/0022024886902058

[38] Abbona F, Christensson F, Angela M and Madsen H 1993 *Journal of Crystal Growth* **131** 331–346 ISSN 00220248 URL http://www.sciencedirect.com/science/article/pii/002202489390183W

[39] Kokubo T and Takadama H 2006 *Biomaterials* **27** 2907–15 ISSN 0142-9612 URL http://www.ncbi.nlm.nih.gov/pubmed/16448693

[40] Bohner M and Lemaitre J 2009 *Biomaterials* **30** 2175–9 ISSN 1878-5905 URL http://www.ncbi.nlm.nih.gov/pubmed/19176246

[41] Rohanová D, Boccaccini A R, Yunos D M, Horkavcová D, Bezovská I and Helebrant A 2011 *Acta biomaterialia* **7** 2623–30 ISSN 1878-7568 URL http://dx.doi.org/10.1016/j.actbio.2011.02.028

[42] Mandel S and Tas A C 2010 *Materials Science and Engineering: C* **30** 245–254 ISSN 09284931 URL http://linkinghub.elsevier.com/retrieve/pii/S0928493109002781

[43] Xie M, Olderø y M O, Andreassen J P, Selbach S M, Strand B L and Sikorski P 2010 *Acta biomaterialia* **6** 3665–75 ISSN 1878-7568 URL http://www.ncbi.nlm.nih.gov/pubmed/20359556

[44] Draget K I, Ø stgaard K and Smidsrø d O 1989 *Applied Microbiology and Biotechnology* **31** ISSN 0175-7598 URL http://link.springer.com/10.1007/BF00252532

[45] Haug A 1964 *Composition and Properties of Alginate* (N.T.H. Trykk)

[46] Strand B L, Gå serød O, Kulseng B, Espevik T, Skjå k Baek G and Skjå k Bræ k G 2002 *Journal of microencapsulation* **19** 615–30 ISSN 0265-2048 URL http://informahealthcare.com/doi/abs/10.1080/02652040210144243http://www.ncbi.nlm.nih.gov/pubmed/12433304

[47] Garside J 1985 *Chemical Engineering Science* **40** 3–26 ISSN 00092509 URL http://www.sciencedirect.com/science/article/pii/0009250985850430

[48] Frawley P J, Mitchell N A, Ó'Ciardhá C T and Hutton K W 2012 *Chemical Engineering Science* **75** 183–197 ISSN 00092509 URL http://linkinghub.elsevier.com/retrieve/pii/S0009250912002114http://www.sciencedirect.com/science/article/pii/S0009250912002114

[49] Rámila A and Vallet-Reg M 2001 *Biomaterials* **22** 2301–2306 ISSN 01429612 URL http://www.sciencedirect.com/science/article/pii/S0142961200004191

[50] Miller M a, Kendall M R, Jain M K, Larson P R, Madden A S and Tas a C 2012 *Journal of the American Ceramic Society* **95** 2178–2188 ISSN 00027820 URL http://doi.wiley.com/10.1111/j.1551-2916.2012.05186.x

[51] Casciani F and Condrate R A 1979 *Spectroscopy Letters* **12** 699–713 ISSN 0038-7010 URL http://www.tandfonline.com/doi/abs/10.1080/00387017908069196

[52] Rehman I and Bonfield W 1997 *Journal of Materials Science: Materials in Medicine* **8** 1–4 ISSN 0957-4530 URL http://link.springer.com/10.1023/A:1018570213546

[53] Westhrin M, Xie M, Olderø y M O, Sikorski P, Strand B L and Standal T 2015 *Plos One* **10** e0120374 ISSN 1932-6203 URL http://dx.plos.org/10.1371/journal.pone.0120374

[54] Olderø y M, Xie M, Westhrin M, Andreassen J p, Zhang Z, Strand B L, Standal T and Sikorski P 2012 *European Cells and Materials* **23, Suppl.** 53

[55] Gryshkov O, Pogozhykh D, Zernetsch H, Hofmann N, Mueller T and Glasmacher B 2014 *Materials science & engineering. C, Materials for biological applications* **36** 77–83 ISSN 1873-0191 URL http://www.sciencedirect.com/science/article/pii/S0928493113006619